EXTENDED EXPERIMENTAL PROCEDURES

Bacterial Strains and Plasmids

The bacterial strains and plasmids used in this study are listed in Tables S1, S2 and S3. Their construction is detailed in Tables S1 and S3, and the oligonucleotides used are listed in Table S4. All plasmids were verified by DNA sequencing. Gene replacement was performed by double homologous recombination using a two-step protocol based on the counter-selectable marker *sacB*. Proper integration of constructs into the *Caulobacter* chromosome was tested by colony PCR.

Growth Conditions and Synchronization

Caulobacter wild-type strain CB15N and its derivatives were grown at 28°C in peptone-yeast-extract (PYE) medium (Poindexter, 1964) or M2-glucose (M2G) minimal medium. To achieve stalk elongation in response to phosphate starvation, stationary cells were diluted 1:20 in $M2G^{-P}$ (Kühn et al., 2010) containing 3.9 mM KCl and cultured for additional 24 hr. Alternatively, cells were directly grown in Hutner imidazole-buffered glucose-glutamate (HIGG) medium containing 30 μM phosphate (Poindexter, 1978). To induce gene expression from the *xylX* promoter (P_{xyl}) (Meisenzahl et al., 1997), medium was supplemented with 0.1% or 0.3% D-xylose. *E. coli* strain TOP10 was used for general cloning purposes. Cells were grown at 37°C in Super Broth (Botstein et al., 1975). Antibiotics were added at the following concentrations (μg ml^{-1}; liquid/solid medium): spectinomycin (25/50), streptomycin (–/5), gentamicin (0.5/5), kanamycin (5/25), ampicillin (-/50) for *Caulobacter* and spectinomycin (50/100), kanamycin (30/50), chloramphenicol (20/30), tetracyline (12/12) for *E. coli*.

Synchronization of *Caulobacter* for microscopy and protein expression analysis was achieved by density gradient centrifugation using Percoll (Tsai and Alley, 2001) or Ludox AS-40 (Sigma-Aldrich) (Ely, 1991), respectively.

Growth Competition Experiments

For short-term competition assays, wild-type, Δ*stpAB* and Δ*stpCD* cells expressing xylose-inducible yellow (YFP) or red (mCherry) fluorescent protein (EK392, EK393, EK416, EK417, EK486, and EK487) were either starved for phosphate (HIGG-30 nM phosphate, 8.9 mM NH_4Cl) or nitrogen (HIGG-200 μM phosphate, 0.4 mM NH_4Cl) in the presence of 0.03% xylose for 3-4 days and mixed at equal optical densities. The exact ratio of wild-type to mutant cells was measured by counting ~1,000 cells by fluorescence microscopy. Cells were resuspended in recovery medium (HIGG-200 μM phosphate, 8.9 mM NH_4Cl) and grown with shaking to late-exponential phase (for 17 hr). The final cell ratio was measured by counting > 1,000 cells by fluorescence microscopy.

For long-term competition assays, mixtures of wild-type and Δ*stpAB* (SW51) or Δ*stpCD* cells (SS250) were repeatedly grown in PYE medium and diluted 1:500 into fresh medium once they had reached stationary phase. The ratio of wild-type to mutant cells was quantified by colony PCR, screening for the absence or presence of the respective mutations. The competition experiments were performed in quintuplicate (Δ*stpAB*) or triplicate (Δ*stpCD)* with independent starting cultures. At least 90 colonies were analyzed per culture and time point.

Immunoblot Analysis

A polyclonal anti-StpA antibody was raised by immunization of rabbits with the StpA-derived peptides 'YPPESPDSGVPHSDEA' (AA 299–314) and 'VSRPPRAAGERPQPRP' (AA 481–496) (Eurogentec). Immunoblot analysis was performed as described previously (Thanbichler and Shapiro, 2006) with anti-StpA, anti-CtrA (Domian et al., 1997), anti-His (Sigma-Aldrich, Germany), anti-GFP (Sigma-Aldrich, Germany), anti-RFP (Chen et al., 2005), anti-SpmX (Radhakrishnan et al., 2008) and anti-StpX (Hughes et al., 2010) rabbit antiserum at dilutions of 1:2,500 (StpA), 1:3,000 (His), 1:10,000 (CtrA, GFP, RFP) or 1:50,000 (SpmX, StpX).

Cell Fractionation Experiments

Biochemical fractionation of cells was performed as described previously (Möll et al., 2010). Cells were cultured in 80 ml PYE to an OD600 of 0.6 and harvested by centrifugation. Pellets were washed in 80 ml 0.2 M Tris-HCl (pH 8) and resuspended in 8 ml 60 mM Tris-HCl (pH 8) containing 0.2 M sucrose, 0.2 mM EDTA, 100 μg/ml PMSF, 5 μg/ml DNaseI and 10 mg/ml lysozyme. The cell suspension was incubated for 10 min at room temperature and frozen in liquid nitrogen. The cells were thawed on ice and lysed by sonication. Cell debris was removed by centrifugation for 10 min at 4,000 g. Subsequently, proteins were fractionated by ultracentrifugation at 100,000 g for 1 hr (4°C). Sedimented membrane proteins were washed in 1 volume 0.2 M Tris-HCl (pH 8) and resuspended in one volume 60 mM Tris-HCl (pH 8) containing 0.2 M sucrose. Protein samples were mixed with 2× SDS sample buffer and analyzed by immunoblotting.

Coimmunoprecipitation and Mass Spectrometric Analysis

Caulobacter strains CB15N (WT) and SS233 (*stpB::stpB*-His) were cultured in 1 l $M2G^{-P}$ for 12 hr. Proteins were crosslinked with 0.6% paraformaldehyde (in 1× PBS, pH 7.4) for 20 min at 28°C. The reaction was quenched with 125 mM glycine (in 1× PBS, pH 7.4) for 5 min at room temperature. Cells were harvested by centrifugation at 8,600 g (4°C) for 10 min and washed with 500 ml 20 mM sodium phosphate buffer (pH 7.4) containing 50 mM NaCl and 1 mM EDTA. Cell pellets were resuspended in BugBuster Protein Extraction Reagent (Novagen, Germany) supplemented with 0.5% n-dodecyl-β-maltoside (Thermo Scientific, USA), 100 μg/ml PMSF and Lysonase Bioprocessing Reagent (Merck, Germany). Complete cell lysis was achieved after two passages

through a French press at 16,000 psi, and cell debris was removed by centrifugation at 16,000 g for 20 min at 4°C. One milliliter of precleared cell lysate was then incubated for 60 min at room temperature with Dynabeads crosslinked to a monoclonal anti-His antibody (SIGMA-Aldrich, Germany). Immobilization of the antibody was carried out as described by the manufacturer. The beads were washed three times with 50 mM Tris-HCl (pH 7.5) containing 150 mM NaCl, 1 mM EDTA, 100 μg/ml PMSF and 0.5% n-dodecyl-β-maltoside, and then with 100 mM Tris-HCl (pH 7.5) containing 750 mM NaCl, 1 mM EDTA and 0.05% n-dodecyl-β-maltoside. Precipitated proteins were eluted from the beads with 400 μl of 0.2% formic acid (pH 2.5) and submitted to mass spectrometric analysis.

Fluorescence Microscopy

For light microscopic analyses, cells were spotted onto pads made of 1% agarose (for still images) or 1% agarose in M2G medium (for time-lapse analyses). When appropriate, the cover slides were sealed with VLAP (vaseline, lanolin and paraffin at a 1:1:1 ratio). Images were recorded with either a Zeiss Axio Imager.M1 microscope equipped with a Plan Apochromat 100×/1.40 Oil DIC objective and a Cascade:1K CCD camera (Photometrics), a Zeiss Axio Imager.Z1 microscope equipped with a 100×/1.46 Oil DIC objective and a pco.edge sCMOS camera (PCO), or a Nikon 90i microscope equipped with a 100×/1.40 Oil phase contrast objective and a Rolera XR CCD camera (QImaging). Images were processed with Metamorph 7.1.2 (Universal Imaging Group) or NIS Elements software (Nikon). Photobleaching experiments were performed with either a 561 nm solid state laser and a 2D-VisiFRAP Galvo System multi-point FRAP module (Visitron Systems, Germany), applying strain-dependent pulses at a laser power of 5%, or a MicroPoint laser system (Photonic Instruments, St. Charles, IL) equipped with an NL100 nitrogen laser (Stanford Research Systems, Sunnyvale, CA) and a 551 nm laser dye. Photobleaching experiments with StpX-GFP were performed with a Leica TCS SP5 scanning confocal microscope equipped with a HCX PL APO Lambda Blue 63×/1.40 Oil objective, a 100 mW argon laser and a 10 mW DPSS laser (Leica Microsystems, Bannockburn, IL). Quantification of photobleaching was performed with ImageJ (NIH) and Matlab (Mathworks).

Transmission Electron Microscopy

Transmission electron micrographs of negatively contrasted *Caulobacter* cells were taken with either a Zeiss CEM902 electron microscope, operated at 80 kV and equipped with a wide-angle dual-speed 2K x 2K CCD camera or a JEOL 2100 electron microscope, operated at 80 kV and equipped with a fast-scan 2K x 2K CCD camera F214. Cells were spotted onto carbon-coated grids (100 mesh) and stained with a 1:2 diluted supernatant of saturated uranyl acetate (in dH20). Image processing and the determination of stalk lengths was carried out with Adobe Photoshop CS2 (Adobe Systems) and the MetaMorph 7.1.2 (Universal Imaging Group) region measurement tool. Statistical significance was assessed with a paired t test with Origin 6.1 (OriginLab).

Electron Cryotomography

Electron cryo-tomography (ECT) was performed as described (Möll et al., 2010). Correlated fluorescence light microscopy (FLM) combined with ECT was essentially carried out as reported previously (Ingerson-Mahar et al., 2010), with the exception that cells were immobilized on C flat 2/2 London finder copper TEM grids with a ~40 nm thick holey carbon coat (Protochips Inc., Raleigh, NC, USA), which were treated with 5 μl of 1 mg/ml sterile-filtered poly-L-lysine (Sigma P1524) before use. The correlative analysis was performed manually with the Adobe Photoshop software (Adobe Systems). The prominent holes in the carbon foil together with the cell body and stalk densities were sufficient to unambiguously overlay the FLM images and the ECT slices. Three-dimensional reconstructions were calculated with IMOD (Mastronarde, 2005), RAPTOR (Amat et al., 2008) or Tomo3D (Agulleiro and Fernandez, 2011). Segmentation and 3D visualization were carried out manually with Amira (Mercury Computer Systems).

SUPPLEMENTAL REFERENCES

Agulleiro, J.I., and Fernandez, J.J. (2011). Fast tomographic reconstruction on multicore computers. Bioinformatics *27*, 582–583.

Amat, F., Moussavi, F., Comolli, L.R., Elidan, G., Downing, K.H., and Horowitz, M. (2008). Markov random field based automatic image alignment for electron tomography. J. Struct. Biol. *161*, 260–275.

Botstein, K., Lew, K.K., Jarvik, V., and Swanson, C.A. (1975). Role of antirepressor in the bipartite control of repression and immunity by bacteriophage P22. J. Mol. Biol. *91*, 439–462.

Chen, J.C., Viollier, P.H., and Shapiro, L. (2005). A membrane metalloprotease participates in the sequential degradation of a *Caulobacter* polarity determinant. Mol. Microbiol. *55*, 1085–1103.

Domian, I.J., Quon, K.C., and Shapiro, L. (1997). Cell type-specific phosphorylation and proteolysis of a transcriptional regulator controls the G1-to-S transition in a bacterial cell cycle. Cell *90*, 415–424.

Ely, B. (1991). Genetics of *Caulobacter crescentus*. Methods Enzymol. *204*, 372–384.

Hughes, H.V., Huitema, E., Pritchard, S., Keiler, K.C., Brun, Y.V., and Viollier, P.H. (2010). Protein localization and dynamics within a bacterial organelle. Proc. Natl. Acad. Sci. USA *107*, 5599–5604.

Ingerson-Mahar, M., Briegel, A., Werner, J.N., Jensen, G.J., and Gitai, Z. (2010). The metabolic enzyme CTP synthase forms cytoskeletal filaments. Nat. Cell Biol. *12*, 739–746.

Kühn, J., Briegel, A., Mörschel, E., Kahnt, J., Leser, K., Wick, S., Jensen, G.J., and Thanbichler, M. (2010). Bactofilins, a ubiquitous class of cytoskeletal proteins mediating polar localization of a cell wall synthase in *Caulobacter crescentus*. EMBO J. *29*, 327–339.

Mastronarde, D.N. (2005). Automated electron microscope tomography using robust prediction of specimen movements. J. Struct. Biol. *152*, 36–51.

Meisenzahl, A.C., Shapiro, L., and Jenal, U. (1997). Isolation and characterization of a xylose-dependent promoter from *Caulobacter crescentus*. J. Bacteriol. *179*, 592–600.

Möll, A., Schlimpert, S., Briegel, A., Jensen, G.J., and Thanbichler, M. (2010). DipM, a new factor required for peptidoglycan remodelling during cell division in *Caulobacter crescentus*. Mol. Microbiol. *77*, 90–107.

Poindexter, J.S. (1964). Biological Properties and Classification of the *Caulobacter* Group. Bacteriol. Rev. *28*, 231–295.

Poindexter, J.S. (1978). Selection for nonbuoyant morphological mutants of *Caulobacter crescentus*. J. Bacteriol. *135*, 1141–1145.

Radhakrishnan, S.K., Thanbichler, M., and Viollier, P.H. (2008). The dynamic interplay between a cell fate determinant and a lysozyme homolog drives the asymmetric division cycle of *Caulobacter crescentus*. Genes Dev. *22*, 212–225.

Thanbichler, M., and Shapiro, L. (2006). MipZ, a spatial regulator coordinating chromosome segregation with cell division in *Caulobacter*. Cell *126*, 147–162.

Tsai, J.W., and Alley, M.R. (2001). Proteolysis of the Caulobacter McpA chemoreceptor is cell cycle regulated by a ClpX-dependent pathway. J. Bacteriol. *183*, 5001–5007.

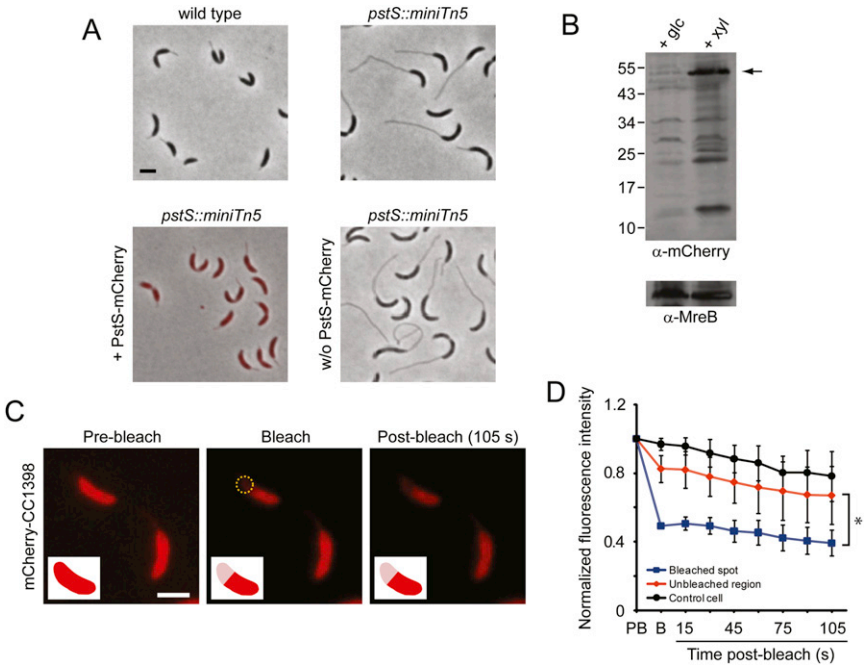

Figure S1. PstS-mCherry Is Functional and FRAP Methodology Can Bleach a Subcellular Region, Related to Figure 1

(A) Functionality of the PstS-mCherry fusion. The indicated strains were grown overnight in PYE and images were captured to assess stalk length. Loss of *pstS* (EK425) leads to stalk elongation as a result of defective phosphate uptake. Xylose-mediated induction of PstS-mCherry (EK424) complements the *pstS* mutant phenotype and reverts the stalks to normal length. Scale bar, 2 μm.

(B) Western blot analysis of strain EK424 showing that the majority of PstS-mCherry is full length (arrow) when cells are grown with 0.3% xylose. The same sample was analyzed with an anti-MreB antibody as a loading control.

(C) FRAP analysis on fixed cells. Cells expressing mCherry-CC1398 (EK61) were fixed in 3.7% formaldehyde to inhibit protein diffusion and analyzed by FRAP. Cells were bleached once where indicated by a dashed circle, followed by a 105 s recovery period. Insets show schematic representations of the results. Note, CC1398 is a so far uncharacterized freely diffusible protein.

(D) Quantification of fluorescence intensities from multiple FRAP experiments (n = 4; *$p < 0.02$; error bars = SD). Cells expressing mCherry-CC1398 were treated as described in (C), and fluorescence intensities were measured in the bleached (blue) and unbleached region (red) of the bleached cell or in the cell body of a nearby control cell (black). To compare the recovery of fluorescence in several cells, the fluorescence intensity of each region of interest was normalized to its pre-bleach intensity. Scale bars, 2 μm.

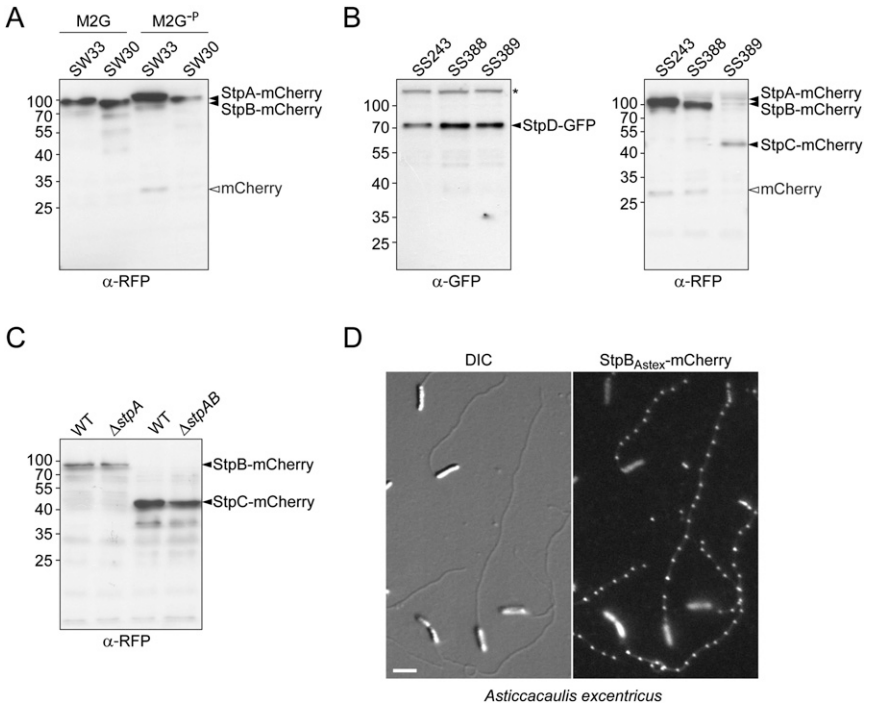

Figure S2. Stability and Cross-Band-like Subcellular Localization of Stp Proteins, Related to Figure 2

(A) Western blot analysis of strain SW33 (P_{xyl}::P_{xyl}-*stpA-mcherry*) and SW30 (P_{xyl}::P_{xyl}-*stpB-mcherry*) cultured for 24h in high-phosphate (M2G) and low-phosphate (M2G^{-P}) medium containing 0.3% xylose to induce production of the fluorescent protein fusions. Filled arrowheads indicate full-length StpA-mCherry or StpB-mCherry. Empty arrowheads point to clipped mCherry.

(B) Western blot analysis of strain SS243 (*stpD::stpD-gfp* P_{xyl}::P_{xyl}-*stpA-mcherry*), SS388 (*stpB::stpB-mcherry stpD::stpD-gfp*) and SS389 (*stpC::stpC-mcherry stpD::stpD-gfp*) showing the stable production of StpD-GFP (left panel) and StpA-mCherry, StpB-mCherry and StpC-mCherry (right panel). Cells were grown in M2G^{-P} for 24h. Synthesis of StpA-mCherrry was induced by adding 0.3% xylose for 24 hr. Samples were analyzed with an anti-GFP and anti-RFP antibody, respectively. Filled arrowheads indicate the full-length fusion proteins. The empty arrowhead points to clipped mCherry. The asterisk denotes a non-specific signal.

(C) Western blot analysis of strains SS412 to SS415 showing the levels of StpB-mCherry and StpC-mCherry when produced from their endogenous promoters in a wild-type or a Δ*stpA* or Δ*stpAB* mutant background. Cells were grown to exponential phase in PYE medium. Samples were probed with an anti-RFP antibody. Filled arrowheads indicate the full-length fusion proteins.

(D) Cells of *Asticcacaulis excentricus* CB48 carrying a mCherry-tagged version of the StpB homolog Astex_0987 (SS309) were cultured in M2G^{-P} and imaged by DIC and fluorescence microscopy. Scale bar, 3 μm.

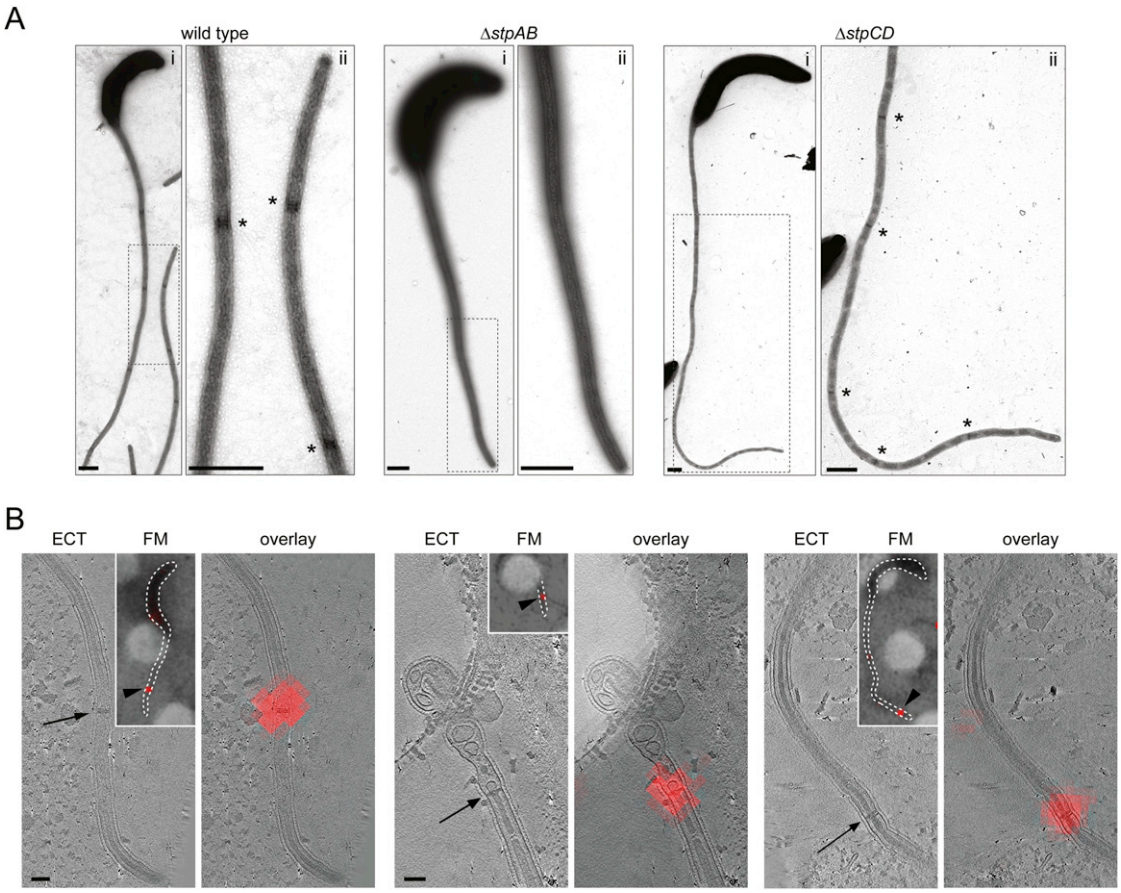

Figure S3. Stp Proteins Are Required for Cross-Band Formation and Colocalize with Cross-Bands, Related to Figure 3

(A) Representative electron micrographs of negatively stained wild-type, Δ*stpAB* (SW51, n = 58) and Δ*stpCD* (SS250, n = 42) cells grown in $M2G^{-P}$ medium. The dashed rectangle in (i) indicates the region magnified in (ii). Asterisks denote cross-bands. Scale bars, 500 nm.

(B) Representative images showing the colocalization of StpB-mCherry with cross-bands (arrows). Cells (SW30) were grown in $M2G^{-P}$ medium with 0.3% xylose and analyzed by correlated fluorescence microscopy (FM) and electron cryo-tomography (ECT). Insets show overlays of phase contrast and fluorescence images, with arrowheads indicating the cross-band visualized in the correlated ECT/FM images (arrows). Scale bars, 100 nm.

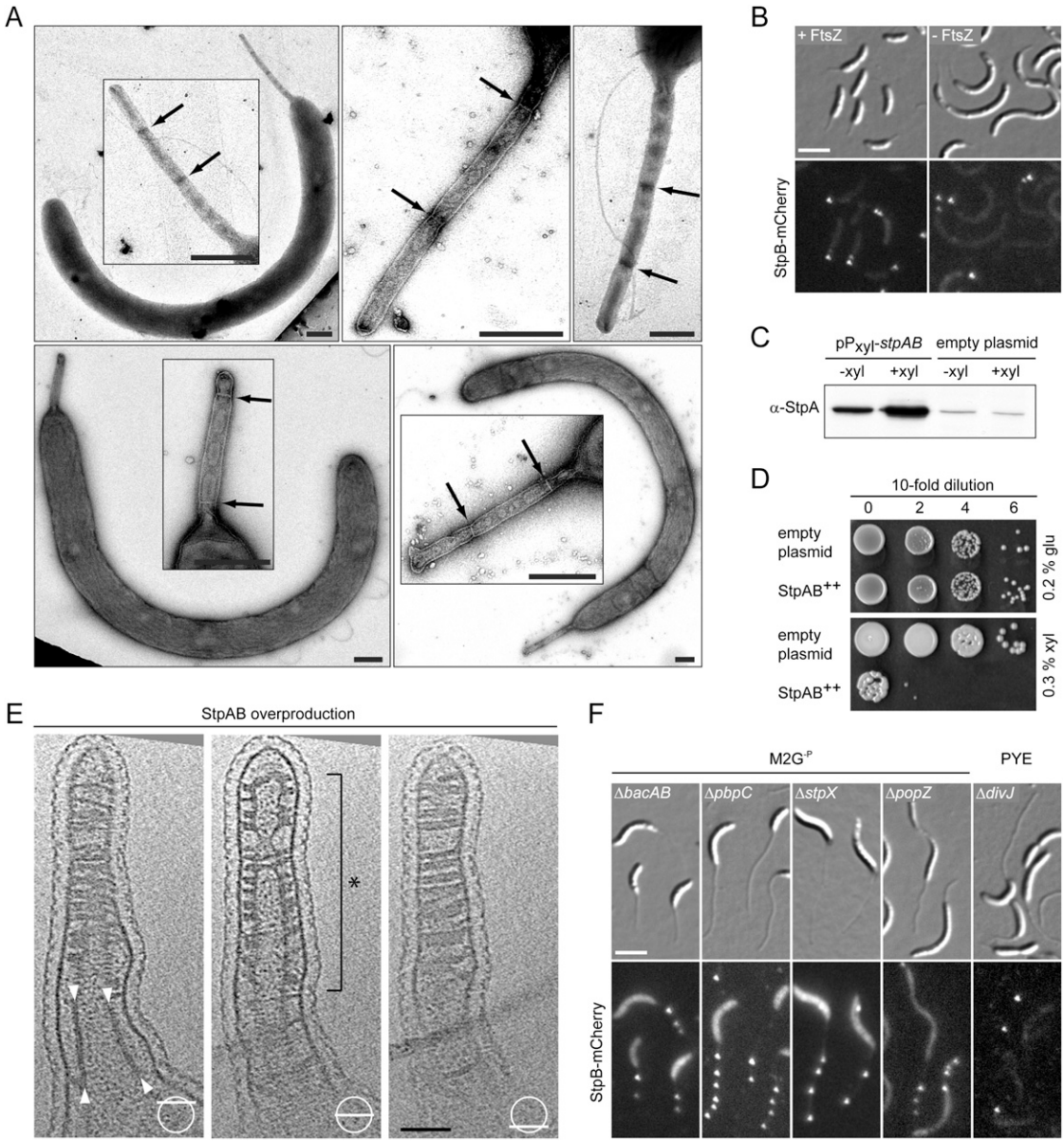

Figure S4. Cross-Band Formation Is Independent of FtsZ and Polar Localizing Proteins, Related to Figure 4

(A) Presence of cross-bands in cells depleted of FtsZ. Swarmer cells of strain SS191 (*ftsZ*::Pxyl-*ftsZ* P_{van}::P_{van}-*stpB-mcherry*) were released into inducer-free M2G medium to suppress FtsZ synthesis, incubated for 6 hr, negatively stained with uranylacetate, and visualized by electron microscopy. Insets show magnifications of the stalks. Arrows point to cross-bands. Scale bars, 500 nm. Note that swarmer cells are largely devoid of FtsZ.

(B) Formation of Stp complexes in the absence of FtsZ. Isolated swarmer cells of strain SS191 (*ftsZ*::Pxyl-*ftsZ* P_{van}::P_{van}-*stpB-mcherry*) were released into M2G medium with and without 0.3% xylose. After 6 hr of incubation, cells were imaged by DIC and fluorescence microscopy. StpB-mCherry production was induced with 0.5 mM vanillate for 2h prior to imaging. Scale bars, 3 μm.

(C) Western blot analysis of cells carrying the *stpAB* overexpression plasmid pP_{xyl}-*stpAB* (SS214) or the corresponding empty plasmid (SS258) showing StpA levels during growth in the absence or presence of 0.3% xylose.

(D) Spot assay showing the viability of strains SS214 (pP_{xyl}-*stpAB*) and SS258 (empty plasmid) upon overproduction of StpAB. Cells were grown in PYE for 24 hr, diluted to an OD600 of 0.16, subjected to the indicated number of serial 10-fold dilutions, and spotted on PYE agar containing either 0.2% glucose or 0.3% xylose.

(E) Representative tomographic slices (top, middle and bottom) through the stalk of a StpAB-overproducing cell. Cells carrying a plasmid-encoded copy of *stpAB* under the control of P_{xyl} (SS214) were pre-cultured in PYE medium and then grown in $M2G^{-P}$ medium containing 0.3% xylose. White arrowheads point to additional densities lining the cytoplasmic membrane. The section used for 3D-reconstruction and image segmentation in Figure 4F and Movie S5 is indicated by an asterisk. Scale bar, 50 nm.

(F) StpB-mCherry shows the normal stalk localization pattern in the absence of BacAB (SS281), PbpC (SS167), StpX (SS213), PopZ (SS292) or DivJ (SS224). Cells were grown for 24 hr in $M2G^{-P}$ medium with 0.3% xylose or to exponential phase in PYE medium with 0.3% xylose. Scale bar, 3 μm.

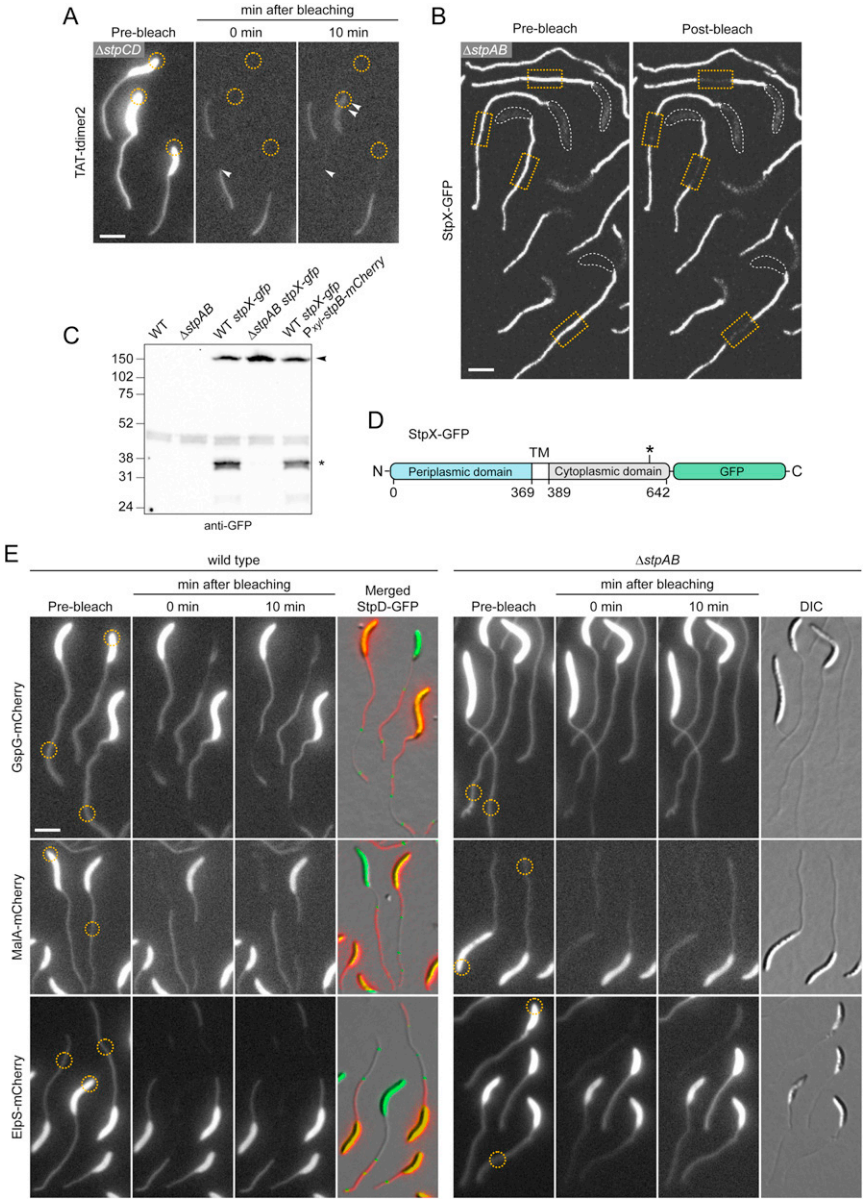

Figure S5. Cross-Bands Act as Protein Diffusion Barriers, Related to Figure 5

(A) The mobility of TAT-tdimer2 was impaired in about 50% of the cells lacking StpC and StpD (SS304). After cells had been grown in $M2G^{-P}$ medium with 0.3% xylose for 24-30 hr and mounted on an agarose pad, the diffusion of TAT-tdimer2 was assessed by FLIP analysis (n = 122 cells). A laser pulse was applied to the regions indicated by a yellow circle. Cells were visualized by DIC and fluorescence microscopy before and after photobleaching. White arrowheads point to a representative cell with a leaky diffusion barrier. Scale bar, 3 μm.

(B) StpX is immobile in StpAB-deficient cells. Cells of a Δ*stpAB* strain expressing StpX-GFP under the control of the native *stpX* promoter (YB5059) were grown in HIGG medium containing 30 μM phosphate, mounted on agarose pads, and subjected to FLIP analysis. Orange rectangles indicate regions that were bleached for 52 s, followed by acquisition of a post-bleach image. Scale bar, 3 μm.

(C) Processing of StpX-GFP is abolished in the absence of cross-bands. Whole-cell lysates of the indicated strains were probed with an anti-GFP antibody (JL-8 monoclonal, Clontech), which detects the cytoplasmic C terminus of the StpX-GFP fusion. The arrowhead indicates the full-length fusion, the asterisk the dominant short fragment.

(D) Schematic of the StpX-GFP fusion used in this study. The asterisk indicates the approximate position of the cleavage site that results in the ~35 kDa cytoplasmic fragment detected by western blot analysis in (C). Numbers indicate the positions of the amino acid residues at the boundaries of the different domains.

(E) FLIP experiments testing the mobility of inducible fluorescent protein fusions to the inner membrane protein GspG and the two outer membrane proteins ElpS and MalA in the presence (SS277, SS283, SS297) and absence (SS272, SS284, SS294) of the Stp complex. Cells were treated as in (A). Yellow circles denote bleached regions. In the overlays shown for wild-type cells producing GspG-mCherry, MalA-mCherry or ElpS-mCherry (red), cross-bands were visualized with a StpD-GFP fusion (green). Scale bar, 3 μm.

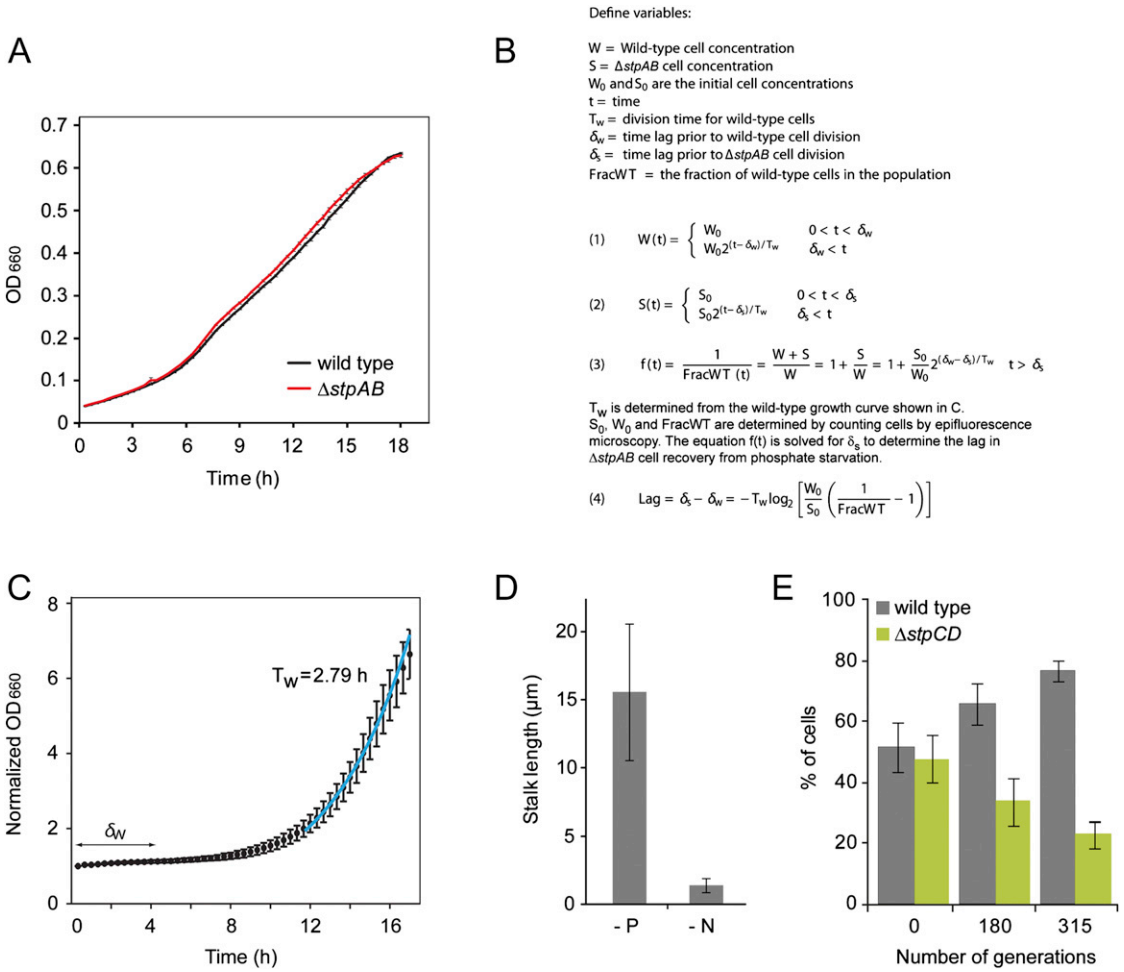

Figure S6. Wild-Type Cells Outcompete Diffusion Barrier-Deficient Mutants, Related to Figure 6

(A) Wild-type and Δ*stpAB* (SW51) cells have equal growth rates. Cells were grown in HIGG-200 μM phosphate (n = 10 for each strain, error bars = SEM). Optical density was monitored over 18 hr in a microplate shaker/reader (Biotek). Note, Δ*stpCD* (SS250) cells show similar growth rates in high-phosphate medium (data not shown).

(B) Equations developed to determine the relative growth lag between wild-type and StpAB-deficient cells after transfer from low-phosphate to phosphate-rich medium. The lag between wild-type and StpCD-deficient cells was determined in an analogous manner.

(C) Determination of the parameters required to solve the equations shown in (B). The doubling time of the wild-type strain was estimated by growing cells overnight in HIGG-30 nM phosphate followed by dilution to an OD_{660} of 0.1 in HIGG-200 μM phosphate. Optical density was monitored over 18 hr in a microplate shaker/reader. The exponential growth rate was determined by fitting the curve to the equation $y = a*2^{t/Tw}$. The fitted line corresponds to a doubling time (Tw) of 2.79 hr.

(D) Stalk lengths measured for wild-type cells (CB15N) after 4 days of phosphate (- P) or nitrogen (- N) starvation (n = 35; error bars = SD).

(E) Wild-type cells outcompete a mutant with leaky diffusion barriers. Wild-type and Δ*stpCD* (SS250) cells were grown in PYE medium and mixed at equal optical densities. The mixed cultures (n = 3) were repeatedly diluted into fresh PYE medium and cultured to stationary phase. At the indicated time points, cells were withdrawn and spread on PYE agar. The ratio of wild-type to barrier-defective cells was determined by colony PCR (n ~360; error bars = SD).